Bioorg. Med. Chem. 40 (2021) 116168

Contents lists available at ScienceDirect

Bioorganic & Medicinal Chemistry

journal homepage: www.elsevier.com/locate/bmc

Novel 4-(piperazin-1-yl)quinolin-2(1*H*)-one bearing thiazoles with antiproliferative activity through VEGFR-2-TK inhibition

Abdelfattah Hassan [a], Mohamed Badr [b], Heba A. Hassan [c,*], Dalia Abdelhamid [c], Gamal El-Din A. Abuo-Rahma [c,d,*]

[a] *Department of Medicinal Chemistry, Faculty of Pharmacy, South Valley University, Qena, Egypt*
[b] *Department of Biochemistry, Faculty of Pharmacy, Menoufia University, Menoufia, Egypt*
[c] *Department of Medicinal Chemistry, Faculty of Pharmacy, Minia University, 61519 Minia, Egypt*
[d] *Department of Pharmaceutical Medicinal Chemistry, Faculty of Pharmacy, Deraya University, New Minia, Minia, Egypt*

ARTICLE INFO

Keywords:
4-Piperazinylquinolin-2(1*H*)-one
4-Phenylthiazole
VEGFR-2 inhibitors
Breast cancer
Angiogenesis

ABSTRACT

A new series of 2-(4-(2-oxo-1,2-dihydroquinolin-4-yl)piperazin-1-yl)-*N*-(4-phenylthiazol-2-yl)acetamide derivatives were synthesized and evaluated for anticancer activity. All target compounds showed anticancer activity higher than that of their 2-oxo-4-piperazinyl-1,2-dihydroquinolin-2(1*H*)-one precursors. Multidose testing of target compounds was performed against breast cancer T-47D cell line. Five compounds showed higher cytotoxic activity than Staurosporine. The dihalogenated derivative showed the best cytotoxic activity with IC_{50} 2.73 ± 0.16 μM. In addition, the VEGFR-2 inhibitory activity of all synthetic compounds was evaluated. Two compounds of 6-fluoro-4-(piperazin-1-yl)quinolin-2(1*H*)-ones showed inhibitory activity comparable to sorafenib with IC_{50} 46.83 ± 2.4, 51.09 ± 2.6 and 51.41 ± 2.3 nM, respectively. The cell cycle analysis of two compounds namely, 2-(4-(6-fluoro-2-oxo-1,2-dihydroquinolin-4-yl)piperazin-1-yl)-*N*-(4-phenylthiazol-2-yl)acetamide and *N*-(4-(4-chlorophenyl)thiazol-2-yl)-2-(4-(2-oxo-1-phenyl-1,2-dihydroquinolin-4-yl)piperazin-1-yl) acetamide revealed that the arrest of cell cycle occurred at S phase. In apoptosis assay, the same two compounds were able to induce significant levels of early and late apoptosis. In a similar manner to Sorafenib, docking of target compounds with VEGFR-2 protein 4ASD showed HB with Cys919 in hinge region of enzyme and HB with both Glu885 and Asp1046 in gate area. Using SwissADME, all target compounds were predicted to be highly absorbed from gastrointestinal tract with no BBB permeability. It is clear that the two compounds are promising antiproliferative candidates that require further optimization.

1. Introduction

One sixth of humankind deaths is due to cancer; cancer rates as the second cause of death worldwide.[1] Breast cancer is by far the most prevalent cancer with about 7.8 million patients worldwide. In females above 40 years, breast cancer has the highest mortality rate that is even more than that of lung cancer.[2] One of the markers of breast malignancy is angiogenesis.[3] Angiogenesis is a stratagem by which tumor expands its own vasculature to guarantee sufficient import of oxygen and nutrients and grow so quickly comparing to normal tissues. This process is fundamental for both tumor growth and metastasis.[4]

Recently, cancer researches focused on drugs that inhibit signaling pathways related to kinases as it is more specific than traditional chemotherapy with fewer adverse effects. Amongst these kinases, the 3 different vascular endothelial growth factor receptors including VEGFR-1, VEGFR-2, and VEGFR-3. VEGFR-2 is the main tyrosine kinase receptor through which Vascular endothelial growth factor VEGF exert its pro-angiogenesis signaling.[5] In addition to angiogenesis, activation of VEGFR-2 triggers a cluster of other cellular events including protease production, vascular permeability, platelet activating factor production, cytoskeleton remodeling, cell survival, proliferation, and migration.[6] The urgent demand of more selective antitumor agents provokes medicinal chemists all over the world to design, develop and evaluate a great number of TK inhibitor candidates. consequently, the majority of FDA approved anticancer medications in last two decades are TK inhibitors with VEGFR-2 inhibitors group as a one of the most effective weapons among all TK inhibitors arsenal.

In spite of a structural diversity of VEGFR-2 inhibitors, they all share

* Corresponding authors at: Department of Medicinal Chemistry, Faculty of Pharmacy, Minia University, 61519 Minia, Egypt (G.E.-D.A. Abuo-Rahma).
E-mail addresses: heba.hasan@mu.edu.eg (H.A. Hassan), gamal.aborahama@mu.edu.eg (G.E.A. Abuo-Rahma).

https://doi.org/10.1016/j.bmc.2021.116168
Received 31 January 2021; Received in revised form 2 April 2021; Accepted 19 April 2021
Available online 22 April 2021

four conclusive pharmacophoric features namely HB heterocycle, spacer, duo HBA/HBD domain and distal hydrophobic moiety (Fig. 3).[7,8] A HB heterocycle is mainly an aromatic or non-aromatic, five or six-membered mono or fused aza-heteroring like pyrazole, indole, thiazole, pyridine, quinoline, quinazoline, phthalazine, benzopyrazole, pyrazolo[3,4-*d*]pyrimidine or benzoxazole.[9–13] Albeit it sometimes can be seven-membered heterocycle like benzodiazepine.[14] Also, HB heterocycle sometimes can be oxa-heteroring as coumarin.[3] HB heterocycle occupies the hinge region of enzyme and interacts with hydrophobic ATP-binding domain and is also capable of forming HB with Cys919 *via* ring nitrogen atom. In addition, the presence of carboxamide or oxo group on α-carbon to nitrogen as in Sorafenib and Sunitinib, respectively adds an extra HB with Cys919 and enhance enzyme inhibition (Fig. 2).[15] A Spacer is a 5-atom length moiety links between HB heterocycle and duo HBD/HBA domain. This spacer is connected to HB heterocycle by nitrogen or oxygen atom.[10,13] Spacer is classically involved in phenyl or heteroring but it can also be incorporated in aliphatic ring or chain.[8,12,16,17] The duo HBA/HBD domain can be urea, thiourea, carboxamide, dicarboxamide, sulfonamide, carbohydrazide, semicarbazone, thiosemicarbazone, *N*-sulfonylurea or even involved in hetero-ring like thiopyrimidinone or pyrazole ring.[8,10,12,17–20] It bonds to both Glu885 and Asp1046 residues in the gate area of enzyme (Fig. 2). Distal hydrophobic moiety occupies an allosteric site of enzyme and it may be variable aliphatic, alicyclic, aromatic, and non-aromatic benzo and heterocyclic groups with diverse electronic, lipophilic, and steric properties.[7,10,12,17,19]

All clinically used VEGFR-2 inhibitors satisfy this well-established four pharmacophoric requirements for good enzyme inhibition. The dual VEGFR/PDGFR inhibitor, Sunitinib and Nintedanib both contain

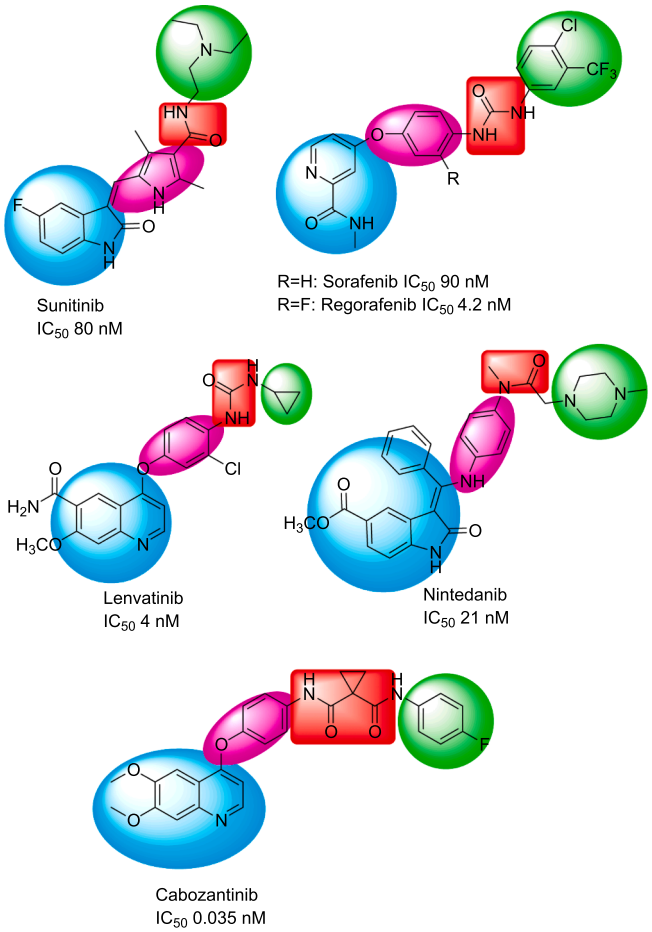

Fig. 1. Some clinically used VEGFR-2 inhibitors.

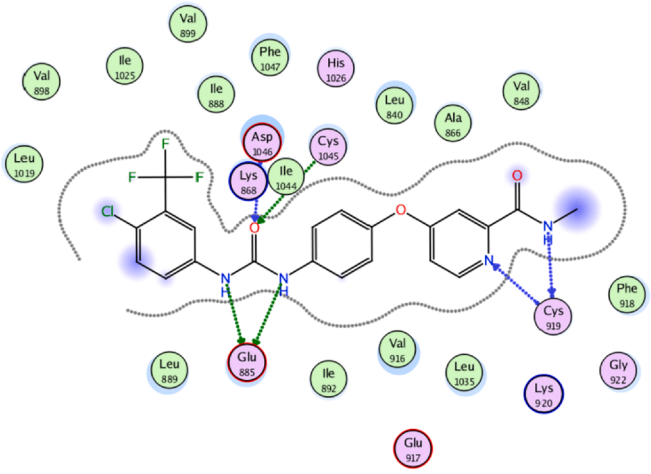

Fig. 2. 2D interactions of sorafenib with VEGFR-2 (PDB: 4ASD).[22]

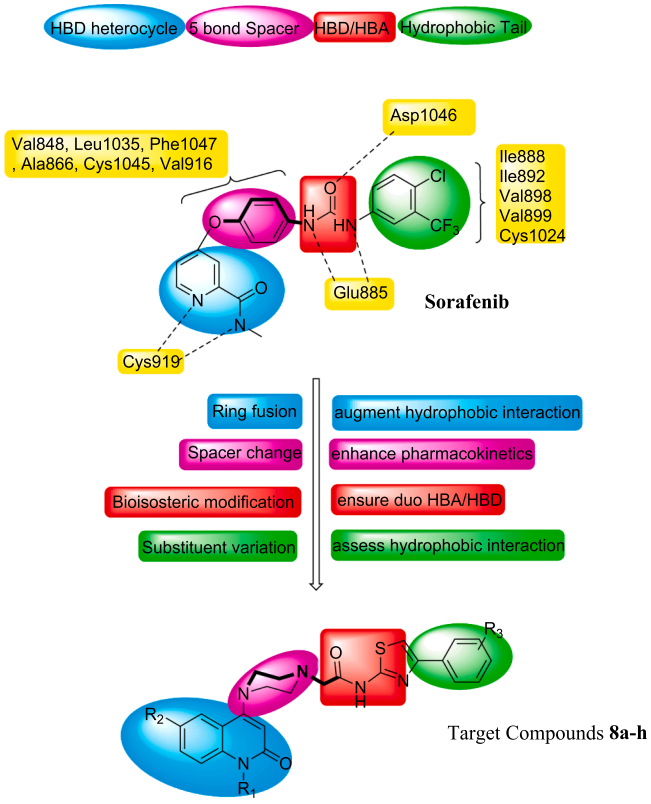

Fig. 3. Pharmacophoric requirements for VEGFR-2 inhibitory activity and design of target compounds **8a-h**.

indolin-2-one as a HB heterocycle and carboxamide as duo HBA/HBD (Fig. 1). Moreover, both drugs have tertiary amine as distal hydrophobic moiety, *N*,*N*-diethylaminoethyl in Sunitinib and 4-methylpiperazinylmethyl in Nintedanib that impacts positively in their pharmacokinetics.[21] Both the dual VEGFR/PDGFR inhibitor, Sorafenib and its fluoro-derivative, the multi-TK inhibitor, Regorafenib have a prototype duo HBA/HBD urea group.[22] Both the multi-TK inhibitor, Cabozantinib and Lenvatinib have quinoline as HB heterocycle. The unique 2-cyclopropylmalondiamide drug, Cabozantinib exerts high VEGFR-2 inhibitory activity at picogram range. Lenvatinib has a characteristic cyclopropyl ring as distal hydrophobic moiety that interacts with an allosteric site of enzyme.[23]

2. Rationale and molecular design

As aforementioned, there are four fundamental pharmacophoric requirements for good VEGFR-2 inhibitory activity namely HB heterocycle, spacer, duo HBA/HBD domain and distal hydrophobic moiety Fig. 3.[7,8] Through ring fusion strategy, the picolinamide ring of Sorafenib was replaced by quinoline-2(1*H*)-one in target compounds which can enhance hydrophobic interaction with hinge region of enzyme.[13] Furthermore, 2-oxo group in quinoline-2(1*H*)-one moiety of target compounds can augment HB with Cys919 like 2-carboxamido group of Sorafenib.[13,15] The length of 5-atom spacer was conserved by replacing oxyphenyl moiety of Sorafenib with more polar piperazinylmethyl moiety that affords additional benefit on pharmacokinetics of target compounds.[16] Regarding to duo HBA/HBD, a bioisosteric modification of urea of Sorafenib to *N*-(thiazol-2-yl)carboxamide moiety enhanced HB with Glu885 and Asp1046 residues in the gate area of enzyme.[12,16,23] Several 4-phenylthiazol-2-yl substituents were incorporated as distal hydrophobic moiety to occupy an allosteric site instead of 3-trifluoromethyl-4-chlorophenyl group of Sorafenib in order to assess the effect of different electron donating and withdrawing substituents on hydrophobic interactions with enzyme.[7,10]

All intermediates **4a,b** and the target final compounds **8a-h** undergone anticancer screening against sixty NCI cell line. In addition, cytotoxicity of target compounds against T-47D breast cancer cell line were evaluated and IC_{50} was calculated and the VEGFR-2 inhibitory activity was assessed for all compounds. For more investigation, the most active compounds in both cytotoxicity and enzyme inhibition **8a** and **8f** were selected for cell cycle analysis and apoptosis assay.

3. Result and discussion

3.1. Chemistry

The synthesis of key intermediates piperazinyl derivatives **4a,b** was sketched in (Scheme 1). The first step is the synthesis of the reported 4-hydroxyquinolin-2(1H)-one derivatives **1a,b** by heating a solution of substituted aniline in diethyl malonate with 5 times by weight PPA at 160 °C for 2 hr.[24] Classically, hydroxyl group of 4-hydroxyquinolin-2(1H)-one was replaced directly with different aliphatic and aromatic amines using neat condition in presence of hydrochloric acid or by heating for long time in a high boiling point solvent like diphenyl ether and DMSO.[25–27] Unfortunately, this direct method did not work with piperazine, so we had to replace the hydroxyl group with a good leaving group -Cl to facilitate the nucleophilic substitution with piperazine. The compound **3b** was synthesized by heating compound **1b** with phosphorus oxychloride at reflux for 2 h. In contrast to compound **1b**, the reaction of compound **1a** with phosphorus oxychloride produced 2,4-dichloro-6-fluoroquinoline compound **2**.[28] So, we had to hydrolyze the 2-chloro group back to hydroxyl group, this was carried out by heating compound **2** in acetic acid at reflux overnight.[24] 4-Piperazinylquinolin-2(1*H*)-ones **4a,b** were synthesized by heating **3a,b** respectively with 3 equivalents of piperazine in DMF at 80 °C.[29,30] ^{1}H NMR of compounds **4a,b** showed two characteristic signals at δ_H 3.2, 2.8 representing 2 sets of piperazinyl eight protons in addition to presence of two sets of signals of piperazinyl carbons at δ_C 46 and 53 in ^{13}C NMR.

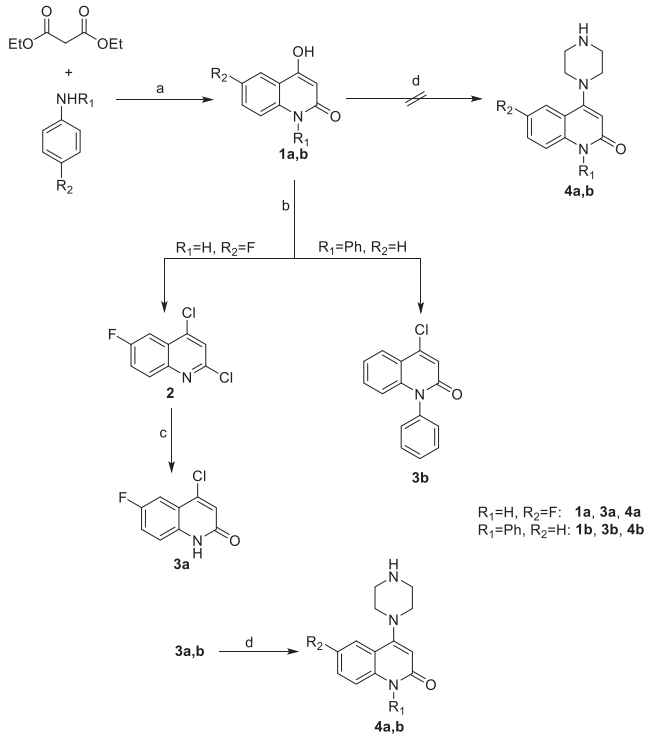

Scheme 1. Synthesis of the intermediates **4a,b**. Reagent and reaction conditions: (a) PPA, 160 °C; (b) $POCl_3$, reflux; (c) AcOH, reflux; (d) piperazine, DMF, 80 °C.

Compounds **7a-d** were synthesized according to reported methods (Scheme 2). Reaction of (us)substituted acetophenones with equivalent amount of *N*-bromosuccinimide (NBS) in presence of *p*-toluene sulfonic acid (*p*-TSA) under neat condition afforded phenacyl bromides **5a-d**.[31] 4-phenylthiazole-2-amines **6a-d** were synthesized by refluxing phenacyl bromides **5a-d** with thiourea in ethanol.[32] acylation of compounds **6a-d** with bromoacetyl bromide in presence of K_2CO_3 yielded compounds **7a-d**.[33] Reaction of compounds **7-d** with key intermediates **4a,b** in DMF in presence of K_2CO_3 afforded target final compounds **8a-h**.[33] ^{1}H NMR of compound **8b**, for example, showed two characteristic NH signals, the first at δ_H 12.13 representing amide CONH and the second at δ_H 11.47 representing quinolinic NH. Moreover, singlet peak at δ_H 3.45 representing methylene group that linked amide and piperazine.

3.2. Biology

3.2.1. NCI evaluation of in vitro antiproliferative activity

Anticancer activity of key intermediate compounds **4a,b** and the target compounds **8a-h** were evaluated by National Cancer Institute (NCI, Bethesda, ML, USA, http://www.dtp.nci.nih.gov.) at a single concentration of 10 μM against a panel of sixty cancer cell lines of nine different human tissues according to NCI protocol. The screening results represent in the precent of growth inhibition of treated cells compared to untreated ones, Table 1. Overall, the quinoline-2(1*H*)-one/thiazole hybrids compounds **8a-h** showed higher cytotoxic activity than their 4-piperazinylquinoline-2(1*H*)-one precursors **4a,b** that reflects the of positive impact of 4-phenylthiazole moiety on anticancer activity of target compounds **8a-h**. Compounds **4a,b** showed weak cell growth inhibition (GI) activity against most of the tested cell line. Most target compounds showed good cytotoxic activity against leukemia cell lines. Compound **8e** exerted good activity against K-562 and MOLT-4 leukemia cell line with GI 77.58% and 82.24%, respectively. For non-small cell lung cancer, target compounds showed inhibition activity against EKVX cell line and compound **8f** is the best with GI 57.30%. Compound **8e** exerted inhibition activity against colon HCT-15 cell line with GI 74.80%. In addition, compound **8e** showed good activity against colon HCT-15 cell line with GI 74.80%. Compound **8b** exerted inhibition activity against CNS SNB-75 cell line with GI 46.25%. Compound **8f** showed good inhibition against melanoma SK-MEL-5 cell line with GI 94.90%, and against ovarian cancer OVCAR-4 cell line with 80.34%. Furthermore, **8f** showed inhibition against renal cancer UO-31 cell line with 70.52% and good inhibition against MDA-MB-468 cell line with GI 90.39%. Compound **8e** exerted inhibition against prostate cancer PC-3 cell line with GI 67.53%. Generally, it is obvious that the screening results of target compounds **8a-h** demonstrated specific activity against

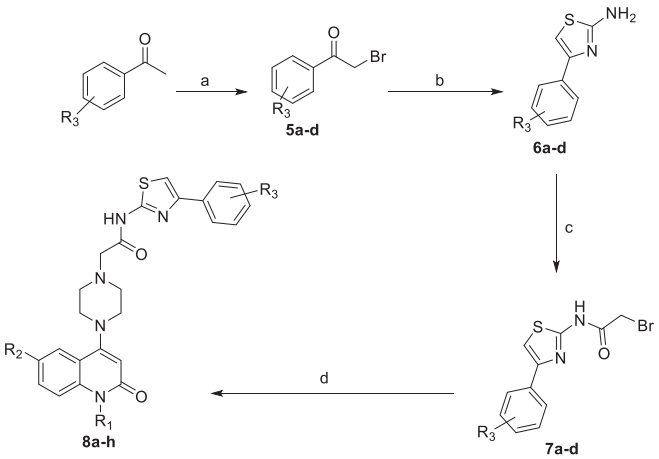

Compound	R_3	Compound	R_1	R_2	R_3	Compound	R_1	R_2	R_3
5a, 6a, 7a	H	**8a**	H	F	H	**8e**	Ph	H	H
5b, 6b, 7b	Cl	**8b**	H	F	Cl	**8f**	Ph	H	Cl
5c, 6c, 7c	Me	**8c**	H	F	Me	**8g**	Ph	H	Me
5d, 6d, 7d	MeO	**8d**	H	F	MeO	**8h**	Ph	H	MeO

Scheme 2. Synthesis of target compounds **8a,h**; Reagent and reaction conditions: (a) NBS, p-TSA, 60–80 °C; (b) thiourea, ethanol, reflux; (c) bromoacetyl bromide, K_2CO_3, 0–5 °C; (d) **3a,b**, K_2CO_3, DMF.

breast cancer cell lines.

3.2.2. Evaluation of in vitro cytotoxicity IC_{50} against breast cancer cell line

NCI in vitro anticancer screening for compounds **4a,b** and **8a-h** demonstrates good antiproliferative activity against breast cancer cell line especially T-47D cell line. Independently, the cytotoxic activity of all synthesized compounds was evaluated against T-47D cell line using MTT assay and the results are presented in (Table 2). All the target compounds showed antiproliferative activity at micromole range. Generally, quinoline-2(1*H*)-one/thiazole hybrid compounds **8a-h** showed prominent higher cytotoxic activity than their corresponding 4-piperazinylquinoline-2(1*H*)-one precursors **4a,b** that is in consistent with the rationale of design and prevents the importance of introducing 4-phenylthiazole moiety in target compounds **8a-h**. Intermediate compounds **4a** and **4b** showed the least cytotoxic activity with IC_{50} 37.70 and 92.1 μM, respectively. Five out of eight target compounds showed higher cytotoxic activity than Staurosporine namely **8a**, **8b**, **8c**, **8e** and **8h**. It is noteworthy that amongst all tested compounds, a dihalogenated derivative **8b** with (R_2 = F and R_3 = Cl) have the best cytotoxic activity with IC_{50} 2.73 μM. In addition, both compounds with unsubstituted 4-phenylthiazole moiety **8a** and **8e** showed higher cytotoxic activity than Staurosporine with IC_{50} 7.20 and 10.30 μM, respectively. Also, compound **8c** with R_3 = Me and **8h** with R_3 = OMe showed higher cytotoxic activity than Staurosporine with IC_{50} 8.41 and 8.11 μM, respectively. Finally, Other three target compounds **8d**, **8f** and **8g** showed comparable cytotoxic activity to Staurosporine with IC_{50} of 16.90, 30.20 and 16.50 μM, respectively.

3.2.3. Evaluation of in vitro cytotoxicity IC_{50} against normal cell line

To assess the selectivity of target compounds **8a-h** against cancer cells over normal ones, the cytotoxicity of two selected compounds **8a** and **8f** was evaluated against non-tumorigenic epithelial cell line, MCF 10A using Camptothecin as a reference Table 3. Two compounds **8a** and **8f** showed less toxicity against normal cell line MCF 10A comparing to Camptothecin. Compound **8a** was showed cytotoxic activity against breast cancer cell line T-47D 5.5 times more than cytotoxic activity against normal cell line MCF 10A while Compound **8f** showed cytotoxic activity against breast cancer cell line T-47D two-fold more than cytotoxic activity against normal cell line MCF 10A.

3.2.4. VEGFR-2 inhibitory assay

To go deeper in molecular mechanism of the synthesized compounds, their inhibitory activity on VEGFR-2 TK was investigated (Table 4). All compounds showed their inhibitory activity at nanomole range. Overall, intermediate compounds **4a,b** showed inhibitory activity less than most of the final target hybrid compounds that confirms the importance of 4-phenylthiazole moiety as a distal hydrophobic moiety which occupies the allosteric hydrophobic pocket of kinase. Compounds **8a** and **8d** showed better inhibitory activity compared with sorafenib with IC_{50} 46.83 ± 2.4, 51.09 ± 2.6 and 51.41 ± 2.3 nM, respectively. Also, compound **8f** showed comparable activity to sorafenib with IC_{50} of 62.7 nM. On the other hand, **4a** and **8c** showed the least activity amongst all synthesized series with 281.5 and 295.8 nM, respectively. The results of both cytotoxicity against T-47D breast cancer cell lines and inhibitory activity against VEGFR-2 TK demonstrates that compounds **8a** and **8f** may be promising targeted anticancer agents. Consequently, further studies like cell cycle analysis and apoptosis assay for both compounds are necessary to be carried out.

3.2.5. Cell cycle analysis and apoptosis assay

3.2.5.1. Cell cycle analysis. The cell cycle includes four phases G1, S, G2 and M. Firstly in G1 phase cell enlarges and DNA becomes ready for duplication. In the second stage (S phase), the DNA starts to replicate and chromatid duplicates; The third stage (G2 Phase), the new DNA is repaired with continuous growth and finally in the fourth stage (M phase) nuclear division occurs. The effect of both compounds **8a** and **8f** on cell cycle development and induction of apoptosis in the T-47D cell line was carried out. T-47D cell line was incubated with IC_{50} concentration of compounds **8a** and **8f** for 24 h. Consequently, the cell line was stained with PI/Annexin V and analyzed by flow cytometry using BD FASCC alibur.[28] The found results were presented in Table 5 and Fig. 4. The results indicated that percentage of % Pre-G1 apoptosis induced by **8a** and **8f** on T47D were 43.05% and 25.12%, respectively. A high percent of cell accumulation occurred in S phase in T-47D cell line treated with compound **8a** and **8f** after 24 h incubation, that indicated the arrest of cell cycle at S phase.

3.2.5.2. Apoptosis assay. After treatment of T-47D cell line with compounds **8a** and **8f**, cell cycle analysis showed presence of pre-G1 peak which indicates apoptosis. To ensure the ability of both compounds **8a**

Table 1
Cytotoxic activity represented in % GI for compounds **4a,b** and **8a-h** at a single concentration of 10 μM against a panel of sixty cancer cell lines.

Cell Line	4a	4b	8a	8b	8c	8d	8e	8f	8g	8h
Leukemia										
CCRF-CEM	–	–	–	33.30	47.04	29.81	60.38	49.34	14.79	24.90
HL-60(TB)	–	–	–	38.30	40.59	23.50	62.85	73.75	19.88	30.20
K-562	–	–	–	44.81	42.38	30.08	77.58	75.77	49.33	56.41
MOLT-4	–	–	13.31	52.80	53.25	46.70	82.24	71.01	32.18	53.11
RPMI-8226	–		–	38.30	51.11	40.93	53.84	63.29	NA	NA
SR	–	–	21.19	29.11	47.49	34.71	48.67	43.18	–	11.21
Non-Small Cell Lung Cancer										
A549/ATCC	–	–	–	44.42	43.68	29.51	43.81	47.42	12.01	19.67
EKVX	56.17	–	14.62	43.34	42.13	24.94	54.54	57.30	26.51	35.21
HOP-62	–	–	–	–	–	–	33.55	34.21	–	12.37
HOP-92	–	16.98	10.93	29.71	39.74	25.44	NA	NA	13.81	–
NCI-H226	–	–	–	12.55	11.70	–	51.84	52.59	17.32	18.69
NCI-H23	–	–	–	28.79	21.63	16.62	39.20	50.24	29.72	35.73
NCI-H322M	–	–	–	21.30	18.88	12.64	10.62	10.90	–	12.63
NCI-H460	–	–	–	18.08	21.36	12.51	67.83	45.18	11.09	15.90
NCI-H522	–	–	–	25.94	22.32	21.61	33.50	43.70	22.85	30.42
Colon Cancer										
COLO 205	–	–	–	14.47	10.67	–	39.94	42.68	–	–
HCC-2998	–	–	–	30.90	34.09	15.75	18.24	–	–	–
HCT-116	–	–	15.96	47.97	45.23	15.87	46.60	64.21	20.19	28.86
HCT-15	–	–	–	34.94	37.14	26.59	74.80	60.28	25.99	17.97
HT29	–	–	–	25.57	21.49	22.10	27.04	36.16	–	–
KM12	–	–	–	30.06	13.31	–	36.97	35.31	–	–
SW-620	–	–	–	41.16	36.96	34.58	31.38	25.68	–	–
CNS Cancer										
SF-268	–	–	–	–	14.49	–	20.78	45.54	13.44	12.44
SF-295	–	–	–	20.36	20.31	17.53	33.27	37.44	14.45	22.86
SF-539	–	–	13.31	30.53	32.66	30.52	22.87	23.90	–	–
SNB-19	–	–	–	30.83	–	15.34	14.78	36.04	21.81	24.23
SNB-75	–	–	–	46.25	32.82	23.88	28.39	32.53	–	–
U251	–	–	–	37.33	44.37	30.29	40.83	36.20	–	–
Melanoma										
LOX IMVI	–	–	–	21.79	23.89	20.79	50.55	41.62	12.15	15.03
MALME-3M	–	–	–	43.30	43.48	33.56	30.27	44.89	–	–
M14	–	–	–	30.62	27.46	19.24	26.60	50.22	–	16.11
MDA-MB-435	NA	NA	NA	NA	NA	NA	NA	NA	NA	NA
SK-MEL-2	–	–	–	–	10.22	–	11.09	24.40	–	–
SK-MEL-28	–	–	–	17.31	17.76	13.65	28.76	30.82	–	–
SK-MEL-5	–	–	–	34.61	44.04	25.43	94.71	94.90	13.48	52.99
UACC-257	–	–	–	31.29	37.55	14.54	51.54	72.00	–	27.79
UACC-62	–	–	14.40	32.04	33.85	28.14	36.06	38.47	20.12	31.07
Ovarian Cancer										
IGROV1	–	–	16.09	50.75	52.56	45.64	32.54	34.48	20.22	21.46
OVCAR-3	–	–	–	16.85	–	–	27.49	32.85	–	17.12
OVCAR-4	–	–	–	39.10	30.65	25.13	76.71	80.34	–	70.36
OVCAR-5	–	–	–	–	–	–	–	–	–	–
OVCAR-8	–	–	–	23.98	23.23	17.24	30.17	40.61	–	15.47
NCI/ADR-RES	–	–	–	41.91	38.36	20.48	37.28	45.08	–	–
SK-OV-3	–	–	–	11.94	11.03	10.36	29.25	28.60	–	–
Renal Cancer										
786–0	–	–	10.27	32.81	25.58	19.33	10.70	32.38	–	–
A498	26.00	–	27.87	60.52	56.56	49.86	33.82	59.25	18.61	12.96
ACHN	–	–	–	38.49	44.07	27.66	36.25	44.88	15.06	19.00
CAKI-1	–	–	17.35	55.45	52.56	46.83	38.56	50.38	–	16.09
RXF 393	–	–	–	37.61	21.07	20.30	23.07	33.00	13.19	–
SN12C	–	–	–	36.18	45.06	29.13	17.88	25.91	13.14	16.04
TK-10	–	–	–	34.28	46.32	31.76	–	37.63	–	–
UO-31	–	–	24.23	37.98	35.43	24.92	58.39	70.52	27.04	27.93
Prostate Cancer										
PC-3	–	–	–	45.09	55.90	35.77	67.53	64.97	23.09	27.53
DU-145	–	–	–	41.07	47.37	39.95	27.28	38.44	–	–
Breast Cancer										
MCF7	–	–	–	39.73	33.48	28.40	72.43	79.86	13.53	25.97
MDA-MB-231/ATCC	–	–	–	16.61	19.02	24.53	37.45	25.31	17.37	22.43
HS 578T	19.60	–	–	33.50	41.36	32.85	17.12	–	–	–
BT-549	–	–	–	27.50	21.53	18.62	32.94	53.51	14.37	19.95
T-47D	10.50	–	29.64	73.25	74.31	69.20	83.44	75.69	40.87	60.05
MDA-MB-468	–	–	12.49	51.40	41.54	31.97	86.69	90.39	30.24	55.27

NA: Not Available, (–) activity less than 10.00%.

Table 2
Cytotoxicity represented in IC_{50} μM for compounds **4a, b** and **8a-h** against breast cancer cell lines (T-47D).

Compound	IC_{50} μM*
4a	37.70 ± 2.22
4b	92.10 ± 5.43
8a	7.20 ± 0.43
8b	2.73 ± 0.16
8c	8.41 ± 0.50
8d	16.90 ± 1.34
8e	10.30 ± 0.61
8f	30.20 ± 1.78
8g	16.50 ± 0.97
8h	8.11 ± 0.48
Staurosporine	11.70 ± 0.69

* IC_{50} values are the mean ± SD of three separate experiments.

Table 3
Cytotoxicity represented in IC_{50} μM for compounds **8a** and **8f** against normal cell lines (MCF 10A).

Compound	IC_{50} μM*
8a	39.40 ± 2.60
8f	64.59 ± 4.20
Camptothecin	24.77 ± 1.63

Table 4
Inhibitory activity against VEGFR-2 expressed in *IC_{50} nM.*

Compound	IC_{50} nM
4a	281.50 ± 12.0
4b	111.90 ± 4.9
8a	46.83 ± 2.4
8b	169.70 ± 7.1
8c	295.80 ± 13.2
8d	51.09 ± 2.6
8e	222.60 ± 9.8
8f	62.70 ± 2.5
8g	167.30 ± 6.4
8h	174.50 ± 7.7
Sorafenib	51.41 ± 2.3

*IC_{50} values are the mean ± SD of three separate experiments.

Table 5
Cell cycle analysis results for compound **8a,f**.

Phase	%G0-G1	%S	%G2/M	%Pre-G1
8a/T47D	41.31	52.39	6.30	43.05
8f/T47D	45.69	49.36	4.95	25.12
cont.T47D	52.59	34.62	12.79	2.61

and **8f** to induce apoptosis, cells were stained with Annexin V/PI, incubated for 24 h and analyzed. Analysis of early and late apoptosis showed that compound **8a** was able to induce significant levels of early and late apoptosis percent 2.31% and 27.88%, respectively (Table 6, Fig. 5 and Fig. 6) and necrosis percent was 12.86%. While compound **8f** induce early and late apoptosis percent 4.06% and 11.21%, respectively and necrosis percent was 9.85% (Table 6).

3.3. Molecular modeling studies

Using Molecular Operating Environment (MOE) software version MOE 2014.0901 software, docking simulation of target compounds **8a-h** was performed with co-crystalized VEGFR-2 protein with Sorafenib (**PDB: 4ASD**). Target compounds **8a-h** showed similar fitness to Sorafenib into active site of enzyme. Investigation of different poses of compound **8a** and **8f** revealed their interactions with Cys919, Glu885 and Asp1046 residues which is in consistent with that of Sorafenib (Fig. 2). 2D style of compound **8a** showed that quinoline-2(1*H*)-one formed dual HB with Cys919 via both nitrogen and oxygen (3.5 Å and 2.52 Å, respectively) in competitive ATP-binding site of enzyme in addition to hydrophobic interactions (Fig. 7). Furthermore, Compound **8a** formed HB with Phe918 (2.87 Å) and Asp1046 (2.99 Å). Compound **8f** showed HB with Cys919 via its oxygen atom (2.61 Å) in addition to *pi*-H interaction of quinoline ring with both Gly922 and Leu840. Duo HBA/ABD domain of compound **8f** achieved its full job, exactly like Sorafenib, in forming two HB with Glu885 (2.60 Å and 2.73 Å) and the third with Asp1046 (3.26 Å) in the gate area of enzyme. Piperazine moiety of both compounds **8a** and **8f** subrogated the central phenyl group of Sorafenib to occupy the distance between hinge region and gate area of the enzyme. Exactly like 3-trifluoromethyl-4-chlorophenyl of Sorafenib, 4-phenylthiazole moiety of compound **8a** and **8f** occupied the hydrophobic allosteric site of enzyme that was built by the side chains of Ile888, Leu892, Val898, Val899 and Cys1024 (Fig. 7).[22]

3.4. In silico physicochemical and pharmacokinetic prediction

Away from efficacy and safety, many drug developments failed due to inappropriate pharmacokinetics, so we utilize a free available SwissADME website from the Swiss Institute of Bioinformatics (http://www.swissadme.ch/index.php) to predict different physicochemical and pharmacokinetic parameters of synthesized compounds.

The Brain Or IntestinaL EstimateD permeation (BOILED-Egg) method is a robust model that accurately predict both gastrointestinal absorption and brain accessibility by calculating both the lipophilicity (expressed in WLOGP) and polarity (expressed in TPSA) of selected compounds Fig. 8. All target compounds **8a-h** showed a high GI absorption while sorafenib showed low gastrointestinal absorption, this is due to remarked decrease of lipophilicity (WLOGP 3.02–4.58) of synthesized compounds comparing to sorafenib (WLOGP 6.32) in addition to reasonable polarity of target compounds (TPSA 98.71–109.57 $Å^2$) (Table 7). Furthermore, target compounds **8a-h** does not pass blood brain barrier that confirming their good CNS safety profile.

In bioavailability radar Fig. 9, six physicochemical properties were taken into account namely lipophilicity, size, polarity, solubility, flexibility, and saturation. The molecular weights of all target compounds are below 500 g/mol except *N*-phenyl derivatives **8e-h** have molecular weights above 500 g/mol, which represents the only Lipinski violation in these target compounds. Otherwise, all target compounds satisfy Lipinski rule with zero violation. All synthesized compounds have higher Fraction Csp3 comparing to sorafenib as the aromatic spacer of sorafenib was replaced by piperazine ring that positively impacted on instauration parameter. All target compounds **8a-h** have rotatable bonds (6–8 bond) almost nearly that of sorafenib.[34–36]

4. Conclusion

A new series of 2-(4-(2-oxo-1,2-dihydroquinolin-4-yl)piperazin-1-yl)-*N*-(4-phenylthiazol-2-yl)acetamide derivatives were synthesized and their structures were confirmed with spectral and elemental analyses. NCI anticancer screening of key intermediates **4a,b** and target compounds **8a-h** revealed higher anticancer activity of the later. Moreover, NCI results demonstrated specific cytotoxic activity of target compounds **8a-h** against breast cancer cell line. Consequently, further multidose testing of compounds **4a,b** and **8a-h** was performed against breast cancer T-47D cell line. Compounds **8a**, **8b**, **8c**, **8e** and **8h** showed higher cytotoxic activity than Staurosporine. The dihalogenated derivative **8b** showed the best cytotoxic activity with IC_{50} 2.73 μM. In addition, compounds **8a** and **8d** showed more inhibitory activity than sorafenib with IC_{50} 46.83 and 51.09 nM, respectively. The cell cycle analysis of compounds **8a** and **8f** revealed that the arrest of cell cycle occurred at S

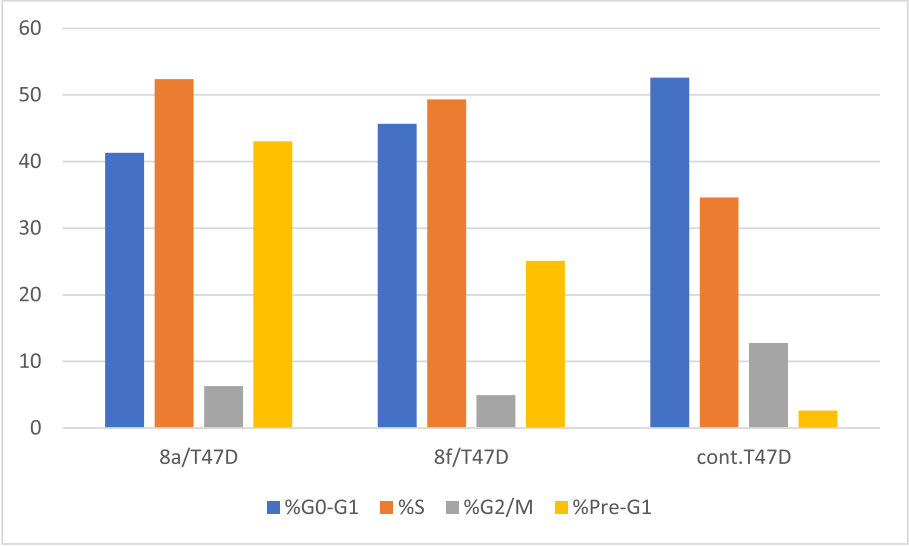

Fig. 4. Cell cycle analysis results for compound **8a,f.**

Table 6
Apoptosis induction analysis using Annexin V/PI for compounds **8a** and **8f**.

code	Apoptosis			Necrosis
	Total	Early	Late	
8a/T47D	43.05	2.31	27.88	12.86
8f/T47D	25.12	4.06	11.21	9.85
cont.T47D	2.61	0.66	0.21	1.74

phase. In apoptosis assay, both compounds **8a** and **8f** were able to induce significant levels of early and late apoptosis. Exactly similar to Sorafenib, docking of target compounds **8a-h** with VEGFR-2 protein 4ASD showed HB with Cys919 in hinge region of enzyme and HB with both Glu885 and Asp1046 in gate area. Using SwissADME, all target compounds **8a-h** were predicted to be highly absorbed from gastrointestinal tract with no BBB permeability. The present study introduces the thiazolyl quinoline-2-one derivatives **8a** and **8f** as promising new antiproliferative candidates that target VEGFR-2 protein and induce apoptosis; theses candidates require *further in vivo,* physicochemical and toxicity optimization.

5. Experimental

5.1. Chemistry

All starting materials were purchased and used without purification. Follow up of reactions was performed by TLC (Kieselgel 60 F_{254}pre-coated plates, Merck, Darmstadt, Germany), the spots were detected by exposure to UV lamp at 254 nm. Melting points were determined on an electrothermal melting point apparatus (Stuart Scientific Co.) and were uncorrected. NMR spectra were measured on a Bruker AV-400 spectrometer at Faculty of Pharmacy, Beni-Suef, Egypt. The ^{1}H and ^{13}C chemical shifts are given relative to internal standard TMS = 0. Coupling constants are stated in Hz. Mass Spectra were performed in Nawah Scientific center, Cairo, Egypt, using APCI as ion source. Elemental analyses for carbon, hydrogen, nitrogen, and sulfur were performed at The Regional Center for Mycology and Biotechnology, Al-Azhar University,

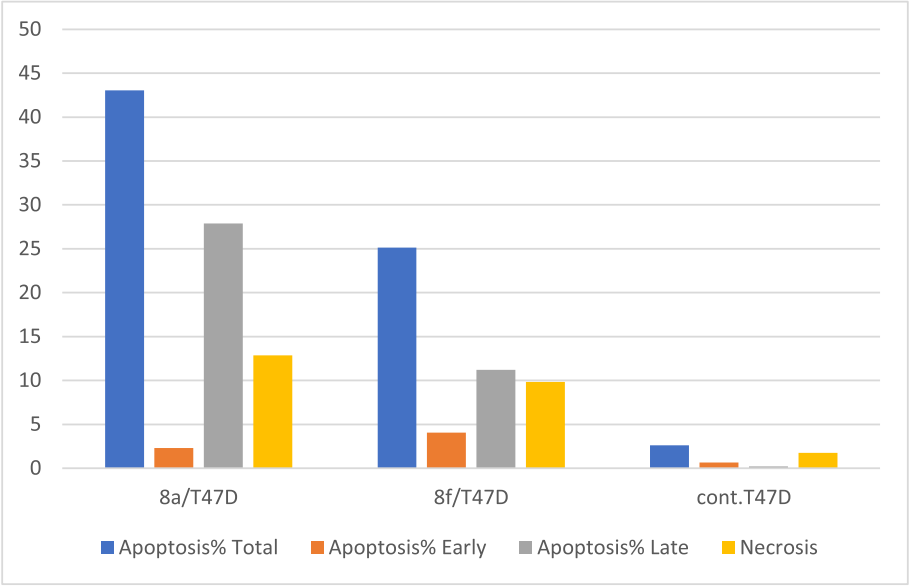

Fig. 5. Apoptosis induction analysis using Annexin V/PI for compounds **8a** and **8f**.

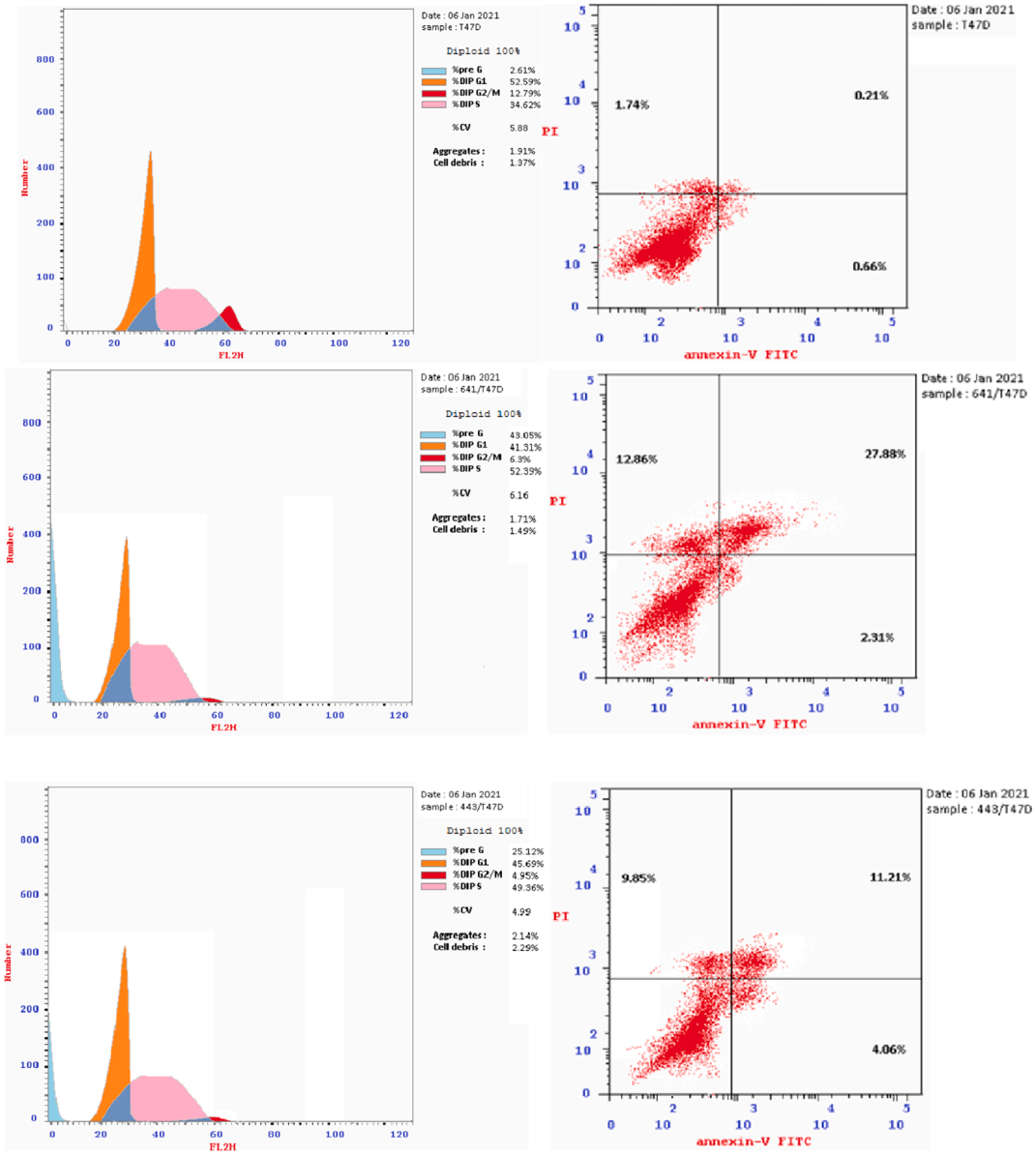

Fig. 6. Apoptosis induction analysis using Annexin V/PI for compound **8a** and **8f.**

Cairo, Egypt. Methods of synthesis and instrumental data of compounds **1a,b**, **2**, **3a,b**, **5a-d**, **6a-d**, and **7a-d** were as reported.[28]

*5.1.1. Synthesis of 4-(piperazin-1-yl)quinolin-2(1H)-one derivatives **4a,b***

A mixture of 10 mmol compound **3a,b**, 30 mmol (0.26 g) piperazine was heated gradually in 10 mL DMF with continuous stirring over 2 h till reach 80 °C then complete heating for another 6 hr. The solution was evaporated under reduced pressure and the residue was triturated with 5% Na_2CO_3 solution, filtered, washed with water, and recrystallized from the appropriate solvent.

*5.1.1.1. 6-Fluoro-4-(piperazin-1-yl)quinolin-2(1H)-one **4a.*** White crystals; yield: 2.10 g (85%); mp: 266–267 °C (ethanol). ^{1}H NMR (400 MHz, DMSO-d_6) δ 11.46 (s, 1H, quin-NH), 7.42–7.29 (m, 3H, quin-Ar–H), 5.91 (s, 1H, quin-C3–H), 2.95 (s, 8H, piperazinyl–H); ^{13}C NMR (101 MHz, DMSO-d_6) δ 163.4, 159.5, 158.4, 156.1, 136.2, 118.8, 117.2, 110.0, 106.9, 52.7, 45.5; TLC-MS: *m/z* calcd: 247.3, found $[M-H]^-$: 246.20. Anal. Calcd for $C_{13}H_{14}FN_3O$ (247.27): C, 63.15; H, 5.7; N, 17. Found: C, 63.2; H, 6.0; N, 16.8.

*5.1.1.2. 1-Phenyl-4-(piperazin-1-yl)quinolin-2(1H)-one **4b.*** White powder; yield: 2.57 g (84%); mp: 203–204 °C (ethanol). ^{1}H NMR (400 MHz, DMSO-d_6) δ 7.83 (d, J = 7.3 Hz, 1H, Ar–H), 7.62 (t, J = 7.4 Hz, 2H, Ar–H), 7.54 (t, J = 7.3 Hz, 1H, Ar–H), 7.40 (t, J = 7.2 Hz, 1H, Ar–H), 7.29 (d, J = 7.3 Hz, 2H, Ar–H), 7.25 (t, J = 7.4 Hz, 1H, Ar–H), 6.57 (d, J = 8.4 Hz, 1H, Ar–H), 6.10 (s, 1H, quin-C3–H), 3.18 (s, 4H, piperazinyl–H), 2.79 (s, 4H, piperazinyl–H); ^{13}C NMR (101 MHz, DMSO-d_6) δ 162.3, 159.4, 141.7, 138.4, 130.7, 130.4, 129.8, 128.9, 125.4, 121.9, 117.1, 116.4, 106.0, 53.3, 46.0; LC-MS: *m/z* calcd: 305.4, found $[M+H]^+$: 306.0. Anal. Calcd for $C_{19}H_{19}N_3O$ (305.38): C, 74.7; H, 6.3; N, 13.8. Found: C, 74.8; H, 6.4; N, 14.0.

*5.1.2. General synthesis of 2-(4-(2-oxo-1,2-dihydroquinolin-4-yl) piperazin-1-yl)-N-(4-phenylthiazol-2-yl)acetamide derivatives **8a-h***

Mixture of compound **4a,b** (1 mmol), appropriate 2-bromo-*N*-(4-phenylthiazol-2-yl)acetamide derivatives **7a-d** (1.1–1.3 mmol) and anhydrous K_2CO_3 (2 mmol, 276 mg) were stirred in 10 mL DMF overnight. The solution was added to crashed ice, filtered, and recrystallized from suitable solvent.

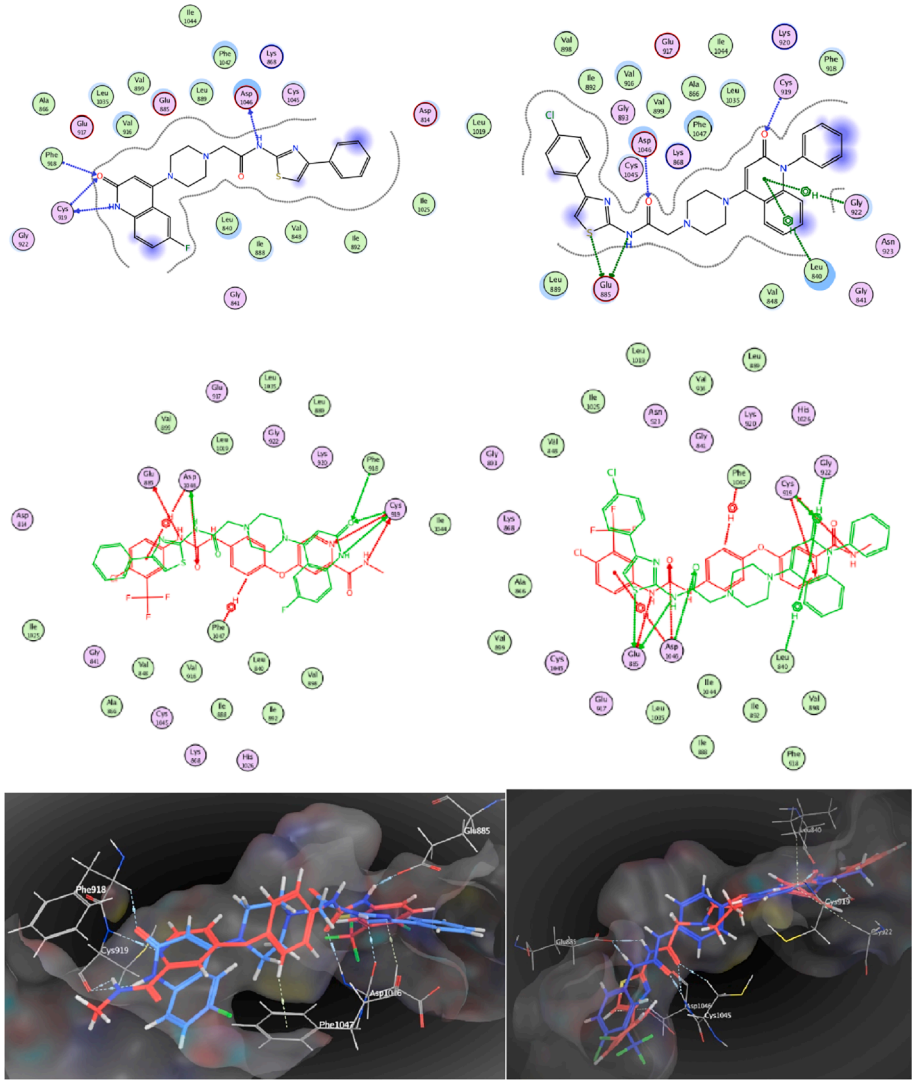

Fig. 7. Docking of compounds **8a** and **8f** with VEGFR-2 (**PDB:4ASD**) illustrating 2D overlaid style (compound in green) with sorafenib (in red) and 3D overlaid style (compound in blue) with sorafenib (in red).

5.1.2.1. 2-(4-(6-fluoro-2-oxo-1,2-dihydroquinolin-4-yl)piperazin-1-yl)-N-(4-phenylthiazol-2-yl)acetamide ***8a.*** White crystals; yield: 370 mg (80%); mp: 263–264 °C. ^{1}H NMR (400 MHz, DMSO-d_6) δ 11.47 (s, 1H, quin-NH), 7.91 (d, J = 7.3 Hz, 2H, Ar–H), 7.66–7.64 (s, 1H, thiazole-Ar–H), 7.46–7.41 (m, 2H Ar–H), 7.39 (dd, J = 8.4, 2.7 Hz, 1H, Ar–H), 7.37–7.30 (m, 3H, quin-Ar–H), 5.97 (s, 1H, quin-C3–H), 3.45 (s, 2H, NHCOCH$_2$), 3.10 (s, 4H, piperazinyl–H), 2.81 (s, 4H, piperazinyl–H); ^{13}C NMR (101 MHz, DMSO-d_6) δ 169.2, 163.0, 158.7, 158.0, 156.0, 149.3, 136.4, 134.7, 129.2, 128.31 126.2, 119.0, 118.3, 117.1, 109.8, 108.6, 107.6, 60.4, 52.7, 51.6; TLC-MS: m/z calcd: 463.5, found [M−H]$^-$: 462.5; Anal. Calcd for $C_{24}H_{22}FN_5O_2S$ (463.53): C, 62.2; H, 4.8; N, 15.1; S, 6.9. Found: C, 62.4; H, 5.1; N, 15.0; S, 6.8.

5.1.2.2. N-(4-(4-chlorophenyl)thiazol-2-yl)-2-(4-(6-fluoro-2-oxo-1,2-dihydroquinolin-4-yl)piperazin-1-yl)acetamide ***8b.*** White powder; yield: 420 mg (85%); mp: 195–196 °C. ^{1}H NMR (400 MHz, DMSO-d_6) δ 12.13 (s, 1H, CONH), 11.47 (s, 1H, quin-NH), 7.93 (d, J = 8.6 Hz, 2H, Ar–H), 7.71 (s, 1H, thiazole-Ar–H), 7.49 (d, J = 8.6 Hz, 2H, Ar–H), 7.42–7.29 (m, 3H, quin-Ar–H), 5.97 (s, 1H, quin-C3–H), 3.45 (s, 2H, NHCOCH$_2$), 3.10 (s, 4H, piperazinyl–H), 2.81 (s, 4H, piperazinyl–H); ^{13}C NMR (101 MHz, DMSO-d_6) δ 169.2, 162.9, 158.6, 158.1, 156.0, 148.1, 136.5, 133.6, 132.8, 129.2, 127.9, 118.9, 118.4, 117.1, 110.0, 109.4, 107.8, 60.4, 52.7, 51.6. TLC-MS: m/z calcd: 498.0, found [M−H]$^-$: 497.0; Anal. Calcd for $C_{24}H_{21}ClFN_5O_2S$ (497.97): C, 57.9; H, 4.25; N, 14.1; S, 6.4; Found: C, 58.15; H, 4.4; N, 14.0; S, 6.2.

5.1.2.3. 2-(4-(6-fluoro-2-oxo-1,2-dihydroquinolin-4-yl)piperazin-1-yl)-N-(4-(p-tolyl)thiazol-2-yl)acetamide ***8c.*** White powder; yield: 410 mg (86%); mp: 192–194 °C. ^{1}H NMR (400 MHz, DMSO-d_6) δ 12.09 (s, 1H, CONH), 11.47 (s, 1H, quin-NH), 7.80 (d, J = 8.1 Hz, 2H), 7.56 (s, 1H, thiazole-Ar–H), 7.42–7.31 (m, 3H, quin-Ar–H), 7.24 (d, J = 8.0 Hz, 2H, Ar–H), 5.97 (s, 1H, quin-C3–H), 3.45 (s, 2H, NHCOCH$_2$), 3.10 (s, 4H, piperazinyl–H), 2.81 (s, 4H, piperazinyl–H), 2.33 (s, 3H, Ar–CH$_3$); ^{13}C NMR (101 MHz, DMSO-d_6) δ 169.1, 163.0, 158.7, 157.8, 156.0, 149.4, 137.7, 136.4, 132.0, 129.8, 126.1, 119.0, 118.3, 117.2, 110.0, 107.7, 107.6, 60.4, 52.7, 51.6, 21.2; TLC-MS: m/z calcd: 477.6, found [M−H]$^-$: 476.4; Anal. Calcd for $C_{25}H_{24}FN_5O_2S$ (477.56): C, 62.9; H, 5.1; N, 14.7; S, 6.7; Found: C, 63.2; H, 5.3; N, 14.6; S. 6.6.

5.1.2.4. 2-(4-(6-fluoro-2-oxo-1,2-dihydroquinolin-4-yl)piperazin-1-yl)-N-(4-(4-methoxyphenyl)thiazol-2-yl)acetamide ***8d.*** White powder; yield: 400 mg (82%); mp: 190–191 °C. ^{1}H NMR (400 MHz, DMSO-d_6) δ 12.09 (s, 1H, CONH), 11.49 (s, 1H, quin-NH), 7.84 (d, J = 8.7 Hz, 2H), 7.46 (s, 1H, thiazole-Ar–H), 7.43–7.36 (m, 1H, quin-Ar–H), 7.33 (dd, J = 8.8, 5.2 Hz, 2H, Ar–H), 6.99 (d, J = 8.8 Hz, 2H, Ar–H), 5.98 (s, 1H, quin-C3–H), 3.79 (s, 3H, Ar–OCH$_3$), 3.44 (s, 2H, NHCOCH$_2$), 3.09 (s, 4H,

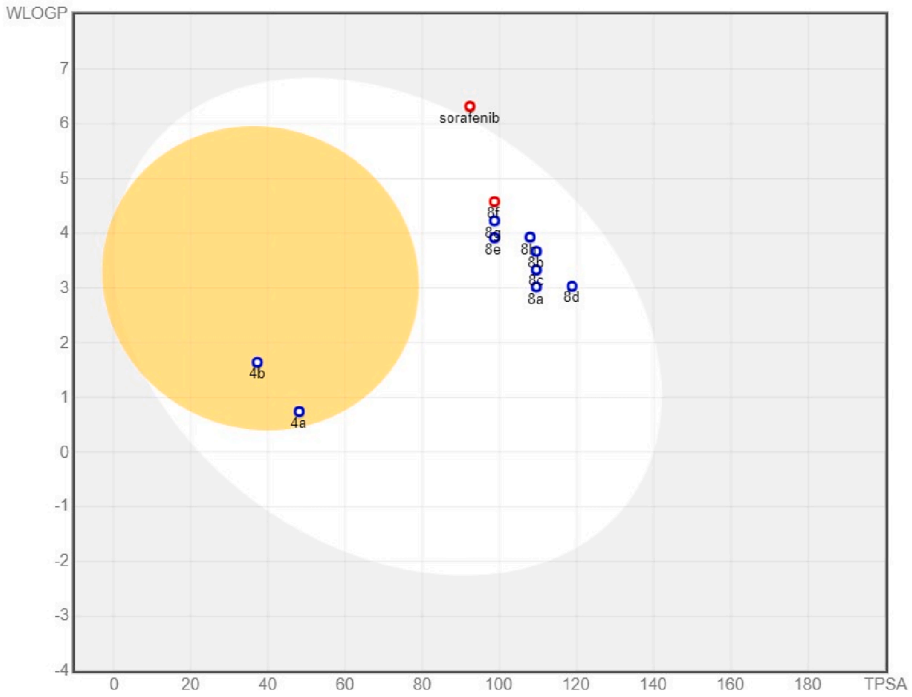

Fig. 8. BOILED Egg plot for sorafenib, compounds **4a,b** and **8a-h**.

Table 7
Swiss ADME physicochemical and pharmacokinetic parameters of sorafenib, compounds **4a,b** and **8a-h**.

Compound	4a	4b	8a	8b	8c	8d	8e	8f	8g	8h	Sorafenib
M.W	247.27	305.37	463.53	497.97	477.55	493.55	521.63	556.08	535.66	551.66	464.82
Fraction Csp3	0.31	0.21	0.21	0.21	0.24	0.24	0.17	0.17	0.19	0.19	0.10
No of rotat.bonds	1	2	6	6	6	7	7	7	7	8	9
No. of HBA	3	2	5	5	5	6	4	4	4	5	7
No. of HBD	2	1	2	2	2	2	1	1	1	1	3
MR	75.89	100.9	135.73	140.74	140.69	142.22	160.75	165.76	165.71	167.24	112.48
TPSA	48.13	37.27	109.57	109.57	109.57	118.8	98.71	98.71	98.71	107.94	92.35
Log P	1.56	2.46	3.2	3.75	3.55	3.17	4.08	4.6	4.39	3.88	4.11
GI absorption	High	High	High	High	High	High	High	High	High	High	Low
BBB permeant	Yes	Yes	No	No	No	No	No	No	No	No	No
Lipin. violations	0	0	0	0	0	0	1	1	1	1	0
Bioavail. Score	0.55	0.55	0.55	0.55	0.55	0.55	0.55	0.55	0.55	0.55	0.55

Fig. 9. Bioavailability radar plot for compounds **8d,e** and sorafenib.

piperazinyl–H), 2.81 (s, 4H, piperazinyl–H); ^{13}C NMR (101 MHz, DMSO-d_6) δ 169.1, 163.1, 159.4, 158.7, 157.8, 156.0, 149.2, 136.4, 127.5, 119.0, 118.7, 117.2, 117.1, 114.5, 110.0, 107.5, 106.6, 60.4, 55.6, 52.7, 51.6; TLC-MS: *m/z* calcd: 493.6, found $[M+H]^-$: 493.9; Anal. Calcd for $C_{25}H_{24}FN_5O_3S$ (493.56): C, 60.8; H, 4.9; N, 14.2; S, 6.5. Found: C, 61.0; H, 5.1; N, 13.95; S, 6.4.

5.1.2.5. 2-(4-(2-oxo-1-phenyl-1,2-dihydroquinolin-4-yl)piperazin-1-yl)-N-(4-phenylthiazol-2-yl)acetamide ***8e.*** Yellow powder; yield: 420 mg (80%); mp: 274–276 °C. ^{1}H NMR (500 MHz, DMSO-d_6) δ 12.21 (s, 1H, CONH), 7.92 (d, J = 9.4 Hz, 2H, Ar–H), 7.82 (d, J = 8.1 Hz, 1H, Ar–H), 7.67 (s, 1H, thiazole-Ar–H), 7.61 (t, J = 7.6 Hz, 2H, Ar–H), 7.54 (t, J = 7.4 Hz, 1H, Ar–H), 7.45 (t, J = 7.7 Hz, 2H, Ar–H), 7.39 (t, J = 8.5 Hz, 1H, Ar–H), 7.34 (t, J = 7.4 Hz, 1H, Ar–H), 7.29 (d, J = 7.2 Hz, 2H, Ar–H), 7.24 (t, J = 7.6 Hz, 1H, Ar–H), 6.53 (d, J = 8.5 Hz, 1H, Ar–H), 6.11 (s,

1H, quin-C3–H), 3.49 (s, 2H, NHCOCH$_2$), 3.19 (s, 4H, piperazinyl–H), 2.86 (s, 4H, piperazinyl–H); ^{13}C NMR (126 MHz, DMSO-d_6) δ 169.1, 162.3, 158.8, 158.0, 149.3, 141.7, 138.3, 134.7, 130.8, 130.5, 129.8, 129.2, 129.0, 128.3, 126.2, 125.4, 122.1, 116.9, 116.5, 108.7, 106.4, 60.4, 52.7, 51.8; TLC-MS: *m/z* calcd: 521.6, found $[M+H]^-$: 521.8; Anal. Calcd for $C_{30}H_{27}N_5O_2S$ (521.64): C, 69.1; H, 5.2; N, 13.4; S, 6.15. Found: C, 69.3; H, 5.4; N, 13.2; S, 6.0.

5.1.2.6. N-(4-(4-chlorophenyl)thiazol-2-yl)-2-(4-(2-oxo-1-phenyl-1,2-dihydroquinolin-4-yl)piperazin-1-yl)acetamide ***8f.*** White powder; yield: 470 mg (84%); mp: 265–267 °C. ^{1}H NMR (500 MHz, DMSO-d_6) δ 12.22 (s, 1H, CONH), 7.94 (d, J = 8.6 Hz, 2H, Ar–H), 7.82 (d, J = 9.1 Hz, 1H, Ar–H), 7.73 (s, 1H, thiazole-Ar–H), 7.61 (t, J = 7.6 Hz, 2H, Ar–H), 7.54 (d, J = 7.5 Hz, 1H, Ar–H), 7.51 (d, J = 8.6 Hz, 2H, Ar–H), 7.39 (t, J = 8.5 Hz, 1H, Ar–H), 7.29 (d, J = 7.2 Hz, 2H, Ar–H), 7.24 (t, J = 7.6 Hz, 1H, Ar–H), 6.52 (d, J = 8.6 Hz, 1H, Ar–H), 6.11 (s, 1H, quin-C3–H), 3.49 (s, 2H, NHCOCH$_2$), 3.19 (s, 4H, piperazinyl–H), 2.86 (s, 4H, piperazinyl–H); ^{13}C NMR (126 MHz, DMSO-d_6) δ 169.2, 162.3, 158.8, 158.2, 148.1, 141.7, 138.3, 133.6, 132.7, 130.8, 130.5, 129.8, 129.3, 129.0, 127.9, 125.4, 122.1, 116.9, 116.5, 109.4, 106.4, 60.4, 52.7, 51.8; TLC-MS: *m/z* calcd: 556.1, found $[M-H]^-$: 555.7; Anal. Calcd for $C_{30}H_{26}ClN_5O_2S$ (556.08): C, 64.8; H, 4.7; N, 12.6; S, 5.8. Found: C, 64.9; H, 4.8; N, 12.7; S, 5.9.

5.1.2.7. 2-(4-(2-oxo-1-phenyl-1,2-dihydroquinolin-4-yl)piperazin-1-yl)-N-(4-(p-tolyl)thiazol-2-yl)acetamide ***8g.*** White crystals; yield: 500 mg (84%); mp: 273–275 °C. ^{1}H NMR (400 MHz, CDCl$_3$) δ 10.28 (s, 1H, CONH), 7.72 (d, J = 7.7 Hz, 1H, Ar–H), 7.67 (d, J = 7.4 Hz, 2H, Ar–H), 7.52 (d, J = 7.1 Hz, 2H, Ar–H), 7.45 (d, J = 6.7 Hz, 1H, Ar–H), 7.22 (d, J = 6.9 Hz, 3H, Ar–H), 7.19–7.13 (m, 3H, Ar–H), 7.05 (s, 1H, thiazole-Ar–H), 6.60 (d, J = 8.5 Hz, 1H, Ar–H), 6.23 (s, 1H, quin-C3–H), 3.34 (s, 2H, NHCOCH$_2$), 3.26 (s, 4H, piperazinyl–H), 2.86 (s, 4H, piperazinyl–H), 2.31 (s, 3H, Ar–CH$_3$); ^{13}C NMR (101 MHz, CDCl$_3$) δ 168.1, 163.2, 158.4, 156.9, 150.3, 141.7, 138.0, 137.8, 131.6, 130.2, 129.5, 129.1, 128.8, 126.0, 124.6, 121.7, 117.2, 116.8, 107.4, 107.2, 61.3, 53.6, 51.6, 29.7; LC-MS: *m/z* calcd: 535.7, found $[M+H]^+$: 536.0; Anal. Calcd for $C_{31}H_{29}N_5O_2S$ (535.67): C, 69.5; H, 5.5; N, 13.1; S, 6.0. Found: C, 69.8; H, 5.7; N, 13.0; S, 5.9.

5.1.2.8. N-(4-(4-methoxyphenyl)thiazol-2-yl)-2-(4-(2-oxo-1-phenyl-1,2-dihydroquinolin-4-yl)piperazin-1-yl)acetamide ***8h.*** White crystals; yield: 450 mg (82%); mp: 276–277 °C. ^{1}H NMR (400 MHz, DMSO-d_6) δ 12.10 (s, 1H, CONH), 7.83 (t, J = 9.1 Hz, 3H, Ar–H), 7.61 (t, J = 7.1 Hz, 2H, Ar–H), 7.54 (d, J = 7.2 Hz, 1H, Ar–H), 7.47 (s, 1H, thiazole-Ar–H), 7.39 (t, J = 7.6 Hz, 1H, Ar–H), 7.28 (d, J = 7.2 Hz, 2H, Ar–H), 7.24 (t, J = 7.5 Hz, 1H, Ar–H), 7.00 (d, J = 8.1 Hz, 2H, Ar–H), 6.53 (d, J = 8.2 Hz, 1H, Ar–H), 6.10 (s, 1H, quin-C3–H), 3.79 (s, 3H, Ar–OCH$_3$), 3.48 (s, 2H, NHCOCH$_2$), 3.19 (s, 4H, piperazinyl–H), 2.87 (s, 4H, piperazinyl–H); ^{13}C NMR (101 MHz, DMSO-d_6) δ 169.0, 162.3, 159.5, 158.8, 157.8, 149.2, 141.7, 138.3, 130.8, 130.4, 129.7, 129.0, 127.5, 125.4, 122.1, 117.0, 116.5, 114.6, 106.6, 106.3, 60.4, 55.6, 52.7, 51.8; LC-MS: *m/z* calcd: 551.7, found $[M+H]^+$: 553.10; Anal. Calcd for $C_{31}H_{29}N_5O_3S$ (551.67): C, 67.5; H, 5.3; N, 12.7; S, 5.8. Found: C, 67.8; H, 5.5; N, 12.7; S, 5.6.

5.2. Biological evaluation

5.2.1. NCI antiproliferative assay

The methodology of the NCI procedures for initial anticancer screening was illustrated on website (http://www.dtp.nci.nih.gov). The protocol based on screening of anticancer candidates against sixty cell lines panel derived from nine different human tumors. NCI-60 testing is performed at a single concentration of 10^{-5} M or 15 μg/ml in accordance with the protocol of the Drug Evaluation Branch, National Cancer Institute, Bethesda, USA.

5.2.2. Evaluation of in vitro cytotoxicity IC_{50} against breast cancer cell line

To inspect the effect of the synthesized compounds **4a,b** and **8a-h** on breast cancer cells, MTT assay was performed against T-47D cell line.[37,38]

5.2.3. Evaluation of in vitro cytotoxicity IC_{50} against normal cell line

The cytotoxicity of target compounds **8a** and **8f** on normal cell line MCF 10A was performed using MTT assay.[37,38]

5.2.4. VEGFR-2 inhibitory assay

VEGFR-2 assay was performed for synthesized compounds **4a,b** and **8a-h** by a well-established reported method following the instructions of (BPS VEGFR2(KDR) Kinase Assay Kit Catalog # 40325, bps bioscience, San Diego, U.S.[39]

5.2.5. Cell cycle analysis and apoptotic assay

The effects of both compounds **8f and 8f** on cell cycle development and induction of apoptosis in the T-47D was performed using the Annexin V-FITC Apoptosis Detection Kit (BioVision Research Products, USA).[40]

5.3. Molecular modeling study

The molecular docking studies were achieved using Molecular Operating Environment software version MOE 2014.0901. Firstly, the co-crystalized VEGFR-2 protein with Sorafenib (PDB: 4ASD) was downloaded from https://www.rcsb.org/. A library of target compounds and Sorafenib were drawn and their energy was minimized by Hamiltonian-Force Field-MMFF94x and the force field partial charges for each molecule were calculated.[16] 3D protonation and correction was performed and water removed. Docking was carried out by using Triangle matcher placement and the rescoring function was London dG. The docking methodology was validated by redocking of Sorafenib into the active site of the enzyme and the results revealed an exact alignment as the original one with the same interactions.

5.4. In silico physicochemical and pharmacokinetic prediction

Physicochemical properties and pharmacokinetics prediction of compounds **4a,b** and **8a-h** were performed using SwissADME which is one of different free available services offered from the Swiss Institute of Bioinformatics. BOILED Egg is a plot of TPSA versus WLOGP with the white region represents the highest probability of gastrointestinal absorption, and the yolk region represents the highest probability to BBB permeability. Lipophilicity is expressed in consensus log $P_{o/w}$ which is calculated by SwissADME and it equals the arithmetic mean of the five different log P values predicted by different freely available models namely XLOGP3, MLOGP, SILICOS-IT, iLOGP in addition to their own model WLOGP which also involved in BOILED Egg plot.[41] Bioavailability radar represents six physicochemical properties: lipophilicity (-0.7 < XLOGP3 > +5.0), size (150 g/mol < MV > 500 g/mol), polarity (20 Å^2 <TPSA > 130 Å^2), insolubility (0 < Log S (ESOL) > 6), insaturation (0.25 < Fraction Csp3 > 1.0), and flexibility (0 < no. of rotatable bonds > 9). The central pink hexagon represents the optimum range for all six parameters. Lipinski filter is used to assess the drug-likeness of synthesized compounds (MW ≤ 500, MLOGP ≤ 4.15, N or O ≤ 10, NH or OH ≤ 5).[42,43]

Declaration of Competing Interest

The authors declare that they have no known competing financial interests or personal relationships that could have appeared to influence the work reported in this paper.

Acknowledgment

The authors are grateful to the National Cancer Institute (NCI), Bethesda, MD for performing the anticancer screening for the target compounds over their panel of cell lines. Authors would like to thank Faculty of Pharmacy, Minia University, Minia and Faculty of Pharmacy, South Valley University, Qena, Egypt

Appendix A. Supplementary material

Supplementary data to this article can be found online at https://doi.org/10.1016/j.bmc.2021.116168.

References

1 World Health Organization Fact Sheets; 2021. https://www.who.int/news-room/fact-sheets/detail/cancer [accessed 22 January 2021].
2 International Agency for Research on Cancer; 2021. https://gco.iarc.fr/today/home [accessed 22 January 2021].
3 Ahmed EY, Latif NAA, El-Mansy MF, Elserwy WS, Abdelhafez OM. VEGFR-2 inhibiting effect and molecular modeling of newly synthesized coumarin derivatives as anti-breast cancer agents. *Bioorg Med Chem*. 2020;28(5), 115328.
4 Qin L, Bromberg-White JL, Qian C-N. Opportunities and challenges in tumor angiogenesis research: back and forth between bench and bed. *Adv Cancer Res Vol 113 Elsevier*. 2012:191–239.
5 Shibuya M. Vascular endothelial growth factor (VEGF) and its receptor (VEGFR) signaling in angiogenesis: a crucial target for anti-and pro-angiogenic therapies. *Genes Cancer*. 2011;2(12):1097–1105.
6 Abdalla AN, Qattan A, Malki WH, Shahid I, Hossain MA, Ahmed M. Significance of Targeting VEGFR-2 and Cyclin D1 in Luminal-A Breast Cancer. *Molecules*. 2020;25 (20):22.
7 El-Adl K, El-Helby A-GA, Sakr H, Eissa IH, El-Hddad SS, Shoman FM. Design, synthesis, molecular docking and anticancer evaluations of 5-benzylidenethiazolidine-2, 4-dione derivatives targeting VEGFR-2 enzyme. *Bioorg Chem*. 2020;102, 104059.
8 Mahdy HA, Ibrahim MK, Metwaly AM, et al. Design, synthesis, molecular modeling, in vivo studies and anticancer evaluation of quinazolin-4 (3H)-one derivatives as potential VEGFR-2 inhibitors and apoptosis inducers. *Bioorg Chem*. 2020;94, 103422.
9 Bhanushali U, Rajendran S, Sarma K, et al. 5-Benzylidene-2, 4-thiazolidenedione derivatives: Design, synthesis and evaluation as inhibitors of angiogenesis targeting VEGR-2. *Bioorg Chem*. 2016;67:139–147.
10 El-Adl K, El-Helby AGA, Sakr H, El-Hddad SS. Design, synthesis, molecular docking, and anticancer evaluations of 1-benzylquinazoline-2, 4 (1H, 3H)-dione bearing different moieties as VEGFR-2 inhibitors. Arch Pharm 2020: e2000068.
11 El-Adl K, El-Helby AGA, Sakr H, et al. Design, synthesis, molecular docking, anticancer evaluations, and in silico pharmacokinetic studies of novel 5-[(4-chloro/2, 4-dichloro) benzylidene] thiazolidine-2, 4-dione derivatives as VEGFR-2 inhibitors. *Arch Pharm*. 2020, e2000279.
12 El-Helby AGA, Sakr H, Eissa IH, Abulkhair H, Al-Karmalawy AA, El-Adl K. Design, synthesis, molecular docking, and anticancer activity of benzoxazole derivatives as VEGFR-2 inhibitors. *Arch Pharm*. 2019;352(10):1900113.
13 Kassab AE, El-Dash Y, Gedawy EM. Novel pyrazolopyrimidine urea derivatives: Synthesis, antiproliferative activity, VEGFR-2 inhibition, and effects on the cell cycle profile. *Arch Pharm*. 2020;353(4):1900319.
14 Saleh NM, El-Gaby MS, El-Adl K, Abd El-Sattar NE. Design, green synthesis, molecular docking and anticancer evaluations of diazepam bearing sulfonamide moieties as VEGFR-2 inhibitors. *Bioorg Chem*. 2020;104, 104350.
15 AbdelHaleem A, Mansour AO, AbdelKader M, Arafa RK. Selective VEGFR-2 inhibitors: Synthesis of pyridine derivatives, cytotoxicity and apoptosis induction profiling. *Bioorg Chem*. 2020;103, 104222.
16 Abou-Seri SM, Eldehna WM, Ali MM, Abou El Ella DA. 1-Piperazinylphthalazines as potential VEGFR-2 inhibitors and anticancer agents: synthesis and in vitro biological evaluation. *Eur J Med Chem*. 2016;107:165–179.
17 El-Adl K, Sakr H, Nasser M, Alswah M, Shoman FM. 5-(4-Methoxybenzylidene) thiazolidine-2, 4-dione-derived VEGFR-2 inhibitors: Design, synthesis, molecular docking, and anticancer evaluations. Arch Pharm 2020: e2000079.
18 Dawood DH, Nossier ES, Ali MM, Mahmoud AE. Synthesis and molecular docking study of new pyrazole derivatives as potent anti-breast cancer agents targeting VEGFR-2 kinase. *Bioorg Chem*. 2020;103916.
19 El-Adl K, Ibrahim MK, Khedr F, Abulkhair HS, Eissa IH. N-Substituted-4-phenylphthalazin-1-amine-derived VEGFR-2 inhibitors: Design, synthesis, molecular docking, and anticancer evaluation studies. *Arch Pharm*. 2020, e2000219.
20 Marzouk AA, Abdel-Aziz SA, Abdelrahman KS, et al. Design and synthesis of new 1,6-dihydropyrimidin-2-thio derivatives targeting VEGFR-2: Molecular docking and antiproliferative evaluation. *Bioorg Chem*. 2020;102, 104090.
21 Roth GJ, Binder R, Colbatzky F, et al. Nintedanib: From Discovery to the Clinic. *J Med Chem*. 2015;58(3):1053–1063.
22 Zeidan MA, Mostafa AS, Gomaa RM, et al. Design, synthesis and docking study of novel picolinamide derivatives as anticancer agents and VEGFR-2 inhibitors. *Eur J Med Chem*. 2019;168:315–329.
23 Abd El Hadi SR, Lasheen DS, Soliman DH, Elrazaz EZ, Abouzid KA. Scaffold hopping and redesign approaches for quinazoline based urea derivatives as potent VEGFR-2 inhibitors. *Bioorg Chem*. 2020, 103961.
24 Elbastawesy MA, Ramadan M, El-Shaier YA, Aly AA, Abuo-Rahma GE-DA. Arylidenes of Quinolin-2-one scaffold as Erlotinib analogues with activities against leukemia through inhibition of EGFR TK/STAT-3 pathways. *Bioorg Chem*. 2020;96, 103628.
25 Fiala W, Stadlbauer W. Nucleophilic Chlorination of 3-Formyl-4-hydroxy-quinolin-2 (1H)-ones. *J für Praktische Chemie/Chemiker-Zeitung*. 1993;335(2):128–134.
26 Curd F, Raison C, Rose F. 167. Synthetic antimalarials. Part XVII. Some aminoalkylaminoquinoline derivatives. *J Chem Soc (Resumed)*. 1947::899–909.
27 Refouvelet B, Guyon C, Jacquot Y, et al. Synthesis of 4-hydroxycoumarin and 2, 4-quinolinediol derivatives and evaluation of their effects on the viability of HepG2 cells and human hepatocytes culture. *Eur J Med Chem*. 2004;39(11):931–937.
28 Elbastawesy MA, Aly AA, Ramadan M, et al. Novel Pyrazoloquinolin-2-ones: Design, synthesis, docking studies, and biological evaluation as antiproliferative EGFR-TK inhibitors. *Bioorg Chem*. 2019;90, 103045.
29 Van Tinh D, Stadlbauer W. Synthesis of 5-mono-and 5, 7-diamino-pyrido [2, 3-d]-pyrimidinediones with potential biological activity by regioselective amination. *J Heterocycl Chem*. 2008;45(3):821–829.
30 Viswas RS, Pundir S, Lee H. Design and synthesis of 4-piperazinyl quinoline derived urea/thioureas for anti-breast cancer activity by a hybrid pharmacophore approach. *J Enzyme Inhib Med Chem*. 2019;34(1):620–630.
31 Pravst I, Zupan M, Stavber S. Halogenation of ketones with N-halosuccinimides under solvent-free reaction conditions. *Tetrahedron*. 2008;64(22):5191–5199.
32 Xu Q, Huang L, Liu J, et al. Design, synthesis and biological evaluation of thiazole-and indole-based derivatives for the treatment of type II diabetes. *Eur J Med Chem*. 2012;52:70–81.
33 Aziz HA, Moustafa GA, Abuo-Rahma GEDA, et al. Synthesis and antimicrobial evaluation of new nitric oxide-donating fluoroquinolone/oxime hybrids. *Arch Pharm*. 2021;354(1):2000180.
34 Daina A, Michielin O, Zoete V. SwissADME: a free web tool to evaluate pharmacokinetics, drug-likeness and medicinal chemistry friendliness of small molecules. *Sci Rep*. 2017;7:42717.
35 Daina A, Michielin O, Zoete V. iLOGP: a simple, robust, and efficient description of n-octanol/water partition coefficient for drug design using the GB/SA approach. *J Chem Inf Model*. 2014;54(12):3284–3301.
36 Daina A, Zoete V. A boiled-egg to predict gastrointestinal absorption and brain penetration of small molecules. *ChemMedChem*. 2016;11(11):1117.
37 Denizot F, Lang R. Rapid colorimetric assay for cell growth and survival: modifications to the tetrazolium dye procedure giving improved sensitivity and reliability. *J Immunol Methods*. 1986;89(2):271–277.
38 Carmichael J, DeGraff WG, Gazdar AF, Minna JD, Mitchell JB. Evaluation of a tetrazolium-based semiautomated colorimetric assay: assessment of chemosensitivity testing. *Cancer Res*. 1987;47(4):936–942.
39 VEGFR2(KDR) Kinase Assay Kit Catalog # 40325; http://bpsbioscience.com/vegfr2-kdr-kinase-assay-kit-40325.
40 Annexin V-FITC Apoptosis Detection Kit; https://www.biovision.com/documentation/datasheets/K101.pdf.
41 Wildman SA, Crippen GM. Prediction of physicochemical parameters by atomic contributions. *J Chem Inf Comput Sci*. 1999;39(5):868–873.
42 Lovering F, Bikker J, Humblet C. Escape from flatland: increasing saturation as an approach to improving clinical success. *J Med Chem*. 2009;52(21):6752–6756.
43 Ritchie TJ, Ertl P, Lewis R. The graphical representation of ADME-related molecule properties for medicinal chemists. *Drug Discov Today*. 2011;16(1–2):65–72.